

Strong interplay between magnetic and structural properties in the spin-1/2 chain molecular compound D-F₅PNN

E. Canévet,^{1,2} B. Grenier,^{2,*} Y. Yoshida,³ N. Sakai,⁴ L.-P. Regnault,² T. Goto,^{4,5} Y. Fujii,⁶ and T. Kawai⁷

¹*Institut Laue Langevin, BP 156, 38042 Grenoble Cedex 9, France*

²*SPSMS, UMR-E 9001, CEA-INSAC/UJF-Grenoble I MDN, F-38054 Grenoble Cedex 9, France*

³*Institute of Applied Physics and Microstructure Research Center, University of Hamburg, Jungiusstrasse 11, D-20355 Hamburg, Germany*

⁴*Graduate School of Human and Environmental Studies, Kyoto University, Kyoto 606-8501, Japan*

⁵*2-43-21 Nangou, Otsu, Shiga Pref. 520-0865, Japan*

⁶*Research Center for Development of Far-Infrared Region, University of Fukui, Fukui 910-8507, Japan*

⁷*Department of Applied Quantum Physics, Kyushu University, Fukuoka 812-8581, Japan*

(Received 23 July 2010; published 25 October 2010)

We present elastic and inelastic neutron scattering results on spin-1/2 chain antiferromagnet D-F₅PNN. We show that a structural transition occurs in zero field below $T_c \sim 710$ mK from $C2/c$ space group (uniform chains) to Pc (bond-alternating chains). When applying a magnetic field at 50 mK, the space group gets back to $C2/c$ above $H_{c1} \sim 1$ T. From the dispersion curves of the magnetic excitations measured at $T=50$ mK, we determine the values of the exchange parameters at 0 and 9 T, which evidence that the magnetic field makes the chains evolve from alternating to uniform. This change in behavior can be correlated unambiguously with the field-induced structural transition. These results evidence “mirror” field- and temperature-induced magneto-crystalline transitions.

DOI: [10.1103/PhysRevB.82.132404](https://doi.org/10.1103/PhysRevB.82.132404)

PACS number(s): 75.25.Dk, 61.05.fm, 61.66.Hq, 75.50.Ee

In the last decades, research on quasi-one-dimensional quantum spin systems has been a very active field in solid-state physics, both theoretically and experimentally. More recently, field effects have been particularly focused on, since the application of a magnetic field can bring new behaviors such as magnetization plateaus and field-induced magnetic orderings (FIMOs).¹ The latter behavior concerns quantum antiferromagnets showing a finite energy gap Δ in zero field between the singlet ($S=0$) ground state and the first excited triplet ($S=1$) state.

In absence of spin-lattice coupling, the application of a magnetic field yields in such a system the closure of the energy gap at critical field $H_{c1} \sim \Delta/g\mu_B$ and a transverse magnetic ordering.¹ A Bose-Einstein condensation of magnons is also predicted.¹ These behaviors were indeed observed in isotropic systems such as spin-1/2 ladder IPA-CuCl₃,² spin-1/2 dimer TiCuCl₃,³ and spin-1/2 alternating chain Cu(NO₃)₂·2.5H₂O.⁴ But a sizable gap was later on detected from electron spin resonance in TiCuCl₃, due to some sizable Dzyaloshinski-Moriya interaction.⁵ More generally, any kind of anisotropy is responsible for the nonclosure of the gap, at H_{c1} , as was evidenced in many compounds, e.g., Haldane spin-1 chain NDMAP,⁶ alternating spin-1 chain NTENP,⁷ and spin-3/2 dimer Cs₃Cr₂Br₉.⁸ Applying further a magnetic field makes the system exit from the FIMO phase at a second critical field H_{c2} (often too high to be reachable on standard equipment) above which the system is fully saturated.

Another interesting feature is the magnetoelastic effects that can yield, upon cooling, a dimerization of uniform spin chains. This so-called spin-Peierls (SP) transition gives also rise at low temperature (LT) to a $S=0$ ground state separated from the triplet state by an energy gap.⁹ As an example, let us refer to the extensively studied compound CuGeO₃.¹⁰ In such

a system, the magnetic field effect is different than in the previous systems, since it drives the system into an incommensurate magnetic phase, described in terms of solitons with parallel magnetization, above the critical field at which the gap closes.

The system we focus on in this Brief Report is the antiferromagnetic (AF) spin-1/2 chain organic compound pentafluorophenyl nitronyl nitroxide (F₅PNN).¹¹ This compound differs from the ones mentioned above by its molecular type: the spin 1/2 arises from a delocalized electron on the ONCNO⁻ group of each molecule [see Fig. 1(a)], typical property of the nitronyl nitroxide radicals family.¹² F₅PNN also has the advantage that H_{c2} is rather low and can thus be easily reached, allowing a study in the saturated phase. At room temperature (RT), the chains, running along the **a+c** direction [see Fig. 1(b)], are uniform, for symmetry reasons. However, magnetization and susceptibility measurements¹¹ show that the system is well described below $T=5$ K by the Hamiltonian of an alternating antiferromagnetic Heisenberg chain (AAHC): $H=J\sum_{i=l}^{N/2}(\mathbf{S}_{2i-1}\cdot\mathbf{S}_{2i}+\alpha\mathbf{S}_{2i}\cdot\mathbf{S}_{2i+1})$ with J the AF exchange interaction ($J>0$), α the alternation ratio ($0\leq\alpha\leq 1$), and the sum over the N spins of the chain. Specific-heat measurements evidence a FIMO for $T\leq 0.2$ K, between $H_{c1}\sim 3$ T and $H_{c2}\sim 6.5$ T.¹³ No reason has been presented yet to explain the contradiction between the model of uniform chain expected from the RT structure analysis and the model of AAHC from the magnetic measurements at $T\leq 5$ K. Moreover, the magnetization curve measured at $T=0.5$ K could not be fitted with a unique alternation ratio over the entire field range,¹¹ indicating a field-induced structural distortion.

In this Brief Report, we report neutron-scattering experiments performed on deuterated F₅PNN (D-F₅PNN).¹⁴ At RT, the space group is $C2/c$ with lattice parameters

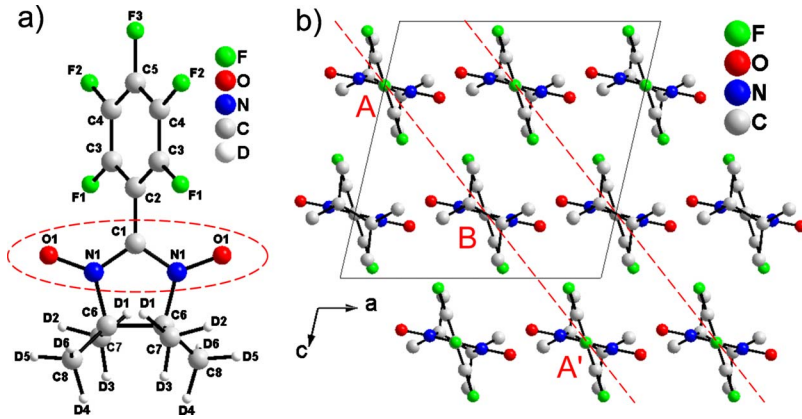


FIG. 1. (Color online) RT structure of D-F₅PNN. (a) Projection of a single molecule in the plane of the ONCNO⁻ group (in the dashed ellipse) on which the unpaired electron is delocalized. (b) Projection along the *b* axis, evidencing the magnetic chains running along *a+c* (dashed lines). For sake of clarity, the deuterium atoms are not represented.

$a=10.918$ Å, $b=11.625$ Å, $c=11.364$ Å, and $\beta=104.06^\circ$.¹⁵ D-F₅PNN is also described by the AAHC model at LT, but with slightly different parameters, as obtained from susceptibility measurements on powder sample: exchange coupling $J=4.84$ K, alternation ratio $\alpha=0.65$, and energy gap $\Delta\approx 0.23$ meV, yielding an expected first critical field H_{c1} of about 1.5 T and a measured second critical field $H_{c2}\approx 6.5$ T.¹⁶

The deuterated single crystal of volume $5\times 5\times 3$ mm³, used both for elastic and inelastic neutron scattering (INS) experiments, was synthesized by Sakai, following the procedure described in Ref. 15. It was previously oriented by Laue x-ray diffraction at CEA-Grenoble, with the *b* axis vertical, and thus the *a-c* plane, containing the chains, horizontal. All neutron-scattering experiments were performed at the high-flux reactor at ILL. The diffraction experiments were performed on the CSIC/CEA-CRG D15 and CEA-CRG D23 single-crystal diffractometers. The D15 experiment was focused on the zero magnetic field study. The sample was mounted in a standard cryostat equipped with a dilution insert, and the diffractometer was operated in the normal-beam mode at a wavelength of 1.175 Å. The D23 experiment was dedicated to the magnetic field dependence of the structure, at a wavelength of 1.28 Å. The sample was placed in a 12 T vertical field cryomagnet ($H\parallel b$) equipped with a dilution insert. The INS experiment was performed on the JCN/CEA-CRG three-axis spectrometer IN12. The sample was placed in a 15 T vertical field cryomagnet ($H\parallel b$) equipped with a dilution insert. The final wave vector \mathbf{k}_f was fixed at 1.1 Å⁻¹ and a Beryllium filter was mounted after the sample.

In order to look for a possible zero-field structural transition occurring below $T=2$ K, we have followed the intensity of various forbidden reflections of space group $C2/c$ as a function of temperature. In decreasing temperature, an increase in intensity was observed below $T=450(50)$ mK on forbidden peaks hkl with $h+k=2n+1$ (n integer), e.g., on $1\ 0\ \bar{1}0$ reflection [see Fig. 2(a)], demonstrating the loss of the *C* centering of the unit cell, and thus a transition toward a lower symmetry space group. Recording an increasing temperature ramp evidenced clear temperature hysteresis, this establishing the first-order character of the transition. To take into account the broadening of this first-order transition, the temperature dependence was fitted by a steplike function convoluted with a Gaussian distribution of critical temperatures, of width ΔT_c [see solid line in Fig. 2]. This yielded a

critical temperature $T_c\sim 710$ mK with $\Delta T_c\sim 150$ mK. Note that the intensity amounts one half of the maximum intensity (I_{\max}) at T_c while it varies between 30% and 70% of I_{\max} on the ΔT_c range around T_c . The other extinction rule, due to the presence of glide *c* mirror, still holds below T_c . Then, we focused on the magnetic field effects on the crystallographic structure at $T=50$ mK. Figure 2(b) shows the field dependence of the integrated intensity of the $1\ 0\ \bar{1}0$ reflection obtained from rocking curves (see inset). Interestingly, this reflection cancels at higher field and thus becomes forbidden again. No satisfactory fit of the field dependence could be obtained so the criteria mentioned above were used to determine H_c ($0.5I_{\max}$) and ΔH_c ($0.3I_{\max}-0.7I_{\max}$): critical fields of about 1.06 and 0.96 T were derived with widths of 0.2 and 0.3 T for increasing and decreasing field, respectively. Here again, a sizable hysteresis is observed.

Last, we have been looking for some magnetic signal at $H=3$ T, located between H_{c1} and H_{c2} , but no magnetic signal could be found on all possible commensurate AF Bragg positions. As a result, either the signal was too small to be detected or the expected FIMO is described by an incommensurate wave vector, unknown so far.

The first step in the investigation was to determine the nuclear structure in zero field at $T=2$ K (above T_c). First, the cell parameters were refined at $T=6$ K: $a=10.807(7)$ Å, $b=11.61(7)$ Å, $c=10.929(7)$ Å, and $\beta=103.20(3)^\circ$. Com-

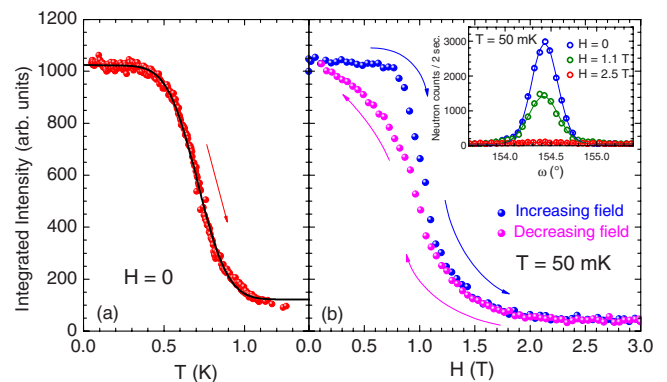


FIG. 2. (Color online) (a) Temperature and (b) field dependence of the $1\ 0\ \bar{1}0$ integrated intensity, measured at $H=0$ for increasing temperature and at $T=50$ mK for increasing and decreasing field, respectively. Inset: rocking curves on the $1\ 0\ \bar{1}0$ reflection for various increasing field values.

paring these parameters to those at RT shows that the compression, upon cooling, occurs mostly along the chain direction. Then, 804 different nuclear reflections (among which 548 independent ones), allowed by the $C2/c$ space group, were collected. The refinement was done with the FULLPROF software¹⁷ and yielded an agreement R_F -factor of 4.18%.¹⁸ Many forbidden peaks were also collected and checked to be null. The $C2/c$ space group yields irrevocably uniform chains (UN chains) since molecule B is symmetrically bordered by molecules A and A' [see Fig. 1(b)] with the following distance between them: $d_{AB}=d_{BA'}=7.009(6)$ Å.¹⁹

The second step was to determine the nuclear structure in zero field at $T=50$ mK $\ll T_c$. The lattice was found to remain monoclinic with no doubling of the cell and the same lattice parameters. Many hkl peaks with $h+k$ odd (forbidden by the C lattice type) were found to be rather strong while all peaks $h0l$ with l odd were found to remain null, confirming the existence of the c mirror perpendicular to the b axis. The loss of the C centering and the dimerization of the chains imply the loss of the twofold axis ($\parallel b$) running through each molecule so that the expected LT space group is Pc . 1425 different reflections allowed in Pc space group (1146 independent ones) were collected. Due to the much larger number of parameters to refine (about four times more), the rigid-body option of the FULLPROF software has been used to refine the structure. Both A and B molecules [see Fig. 1(b)] were described as rigid molecules, using as input the atomic coordinates and isotropic Debye-Waller factors refined at 2 K. That way, the structure below T_c could be refined successfully in the Pc space group with an agreement R_F -factor of 7.78%. The symmetrical position of molecule B between molecules A and A' [see Fig. 1(b)] is lost at the same time than the loss of the C centering and the inversion. Indeed, the distance from molecule A to B and that from molecule B to A' are now: $d_{AB}=7.034(8)$ Å and $d_{BA'}=6.984(8)$ Å,¹⁹ respectively, so that the chains are now dimerized and form alternating (ALT) chains.

Last, 367 reflections (264 independent ones) allowed by $C2/c$ space group (UN chains) were collected at $T=50$ mK and $H=9$ T, in order to refine the nuclear structure in the fully saturated phase. Reflections forbidden by the C centering and the c mirror were also collected and checked to be null. The refinement of the structure has been done with the $C2/c$ space group, yielding an agreement R_F -factor of 4.68% with the same crystallographic structure as the one found at $T=2$ K and zero field.

We now present the INS results obtained on IN12. We have measured at 40 mK the dispersion of magnetic excitations along the chain direction ($\mathbf{a}+\mathbf{c}$) at $H=0$ T (gapped phase) and $H=9$ T (fully saturated phase). Typical background subtracted constant- Q energy scans are shown in the inset of Fig. 3 for various $\mathbf{Q}=(h0h)$ scattering vectors at $H=0$. It is worth noting that the scan performed at the AF point ($h=1/2$) is larger than the resolution. It was thus fitted by two resolution-limited Gaussian functions, yielding $\Delta_- = 0.17(1)$ meV and $\Delta_+ = 0.22(1)$ meV, evidencing a small splitting of the triplet state. The reason for that could come from the nature of the spin 1/2, a delocalized electron, yielding some spin-orbit coupling or Dzyaloshinski-Moriya interaction. The dispersion curves deduced from such scans at

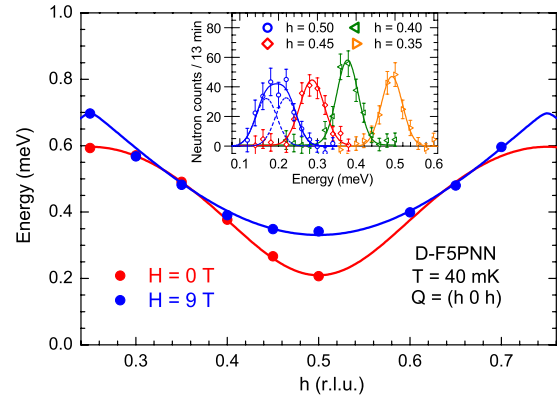


FIG. 3. (Color online) Dispersion curves of the magnetic excitations at $H=0$ and 9 T for $H\parallel b$, measured along the chain direction (closed symbols). The solid lines are fit to the data (see text). Inset: background-subtracted constant- Q energy scans measured at $H=0$ (empty symbols) and fitted by one or two Gaussian function(s) (solid lines).

$H=0$ and 9 T are depicted in Fig. 3. The positions of the points were extracted from Gaussian fit of the energy scans. In zero field, the obtained branch is that of the (quasi)degenerated triplet excitations whereas at $H=9$ T, it corresponds to the lowest energy branch. Neglecting, at first order, the interchain couplings, the dispersion curve at $H=0$ was fitted using the relation derived from perturbation theory on α for spin-1/2 AAHC (Ref. 20): $E(h) = J \sum_{n=0}^3 A_n(\alpha) \cos(4n\pi h)$ where the $A_n(\alpha)$ are third-order polynomial functions of the alternation ratio α . The dispersion curve could be well fitted, yielding $J=4.99(6)$ K and $\alpha=0.66(2)$.

At $H=9$ T (fully saturated phase), the spin-wave dispersion curve can be easily calculated. The two following dispersion curves were derived: $E^\pm(h, H) = g\mu_B H - SJ(1+\alpha) \pm SJ\sqrt{1+2\alpha \cos 4\pi h + \alpha^2}$, but only the lowest branch was observed. The fit yields $J=4.2(2)$ K and $\alpha=1.00(8)$. Interestingly, D-F₅PNN is described by a uniform AF chain system ($\alpha=1$), as it was above T_c in zero field. Note also that the exchange coupling of 4.2 K at 9 T corresponds precisely to the average between the zero-field couplings, $J=4.99$ K and $J' = \alpha J = 3.29$ K.

Let us now conclude on these complementary results on the crystallographic structure and the magnetic excitations in the various phases. First of all, the temperature-driven dimerization of the chains evidenced in zero field explains unequivocally the alternating character of the magnetic couplings at LT with couplings $J_{AB}=J > J_{BA'} = \alpha J$. Moreover, the change in behavior at $T=50$ mK from alternating chain in zero field to uniform chain in high field can unambiguously be correlated with the crystallographic field-induced transition observed at $H_{c1} \sim 1$ T, from Pc (ALT chains) to $C2/c$ (UN chains) space group. We can anticipate that the measurement of the dispersion curve at a magnetic field slightly larger than H_{c1} would already give a uniform chain behavior since the chains are no longer dimerized.

Last, we wish to discuss on the nature of these temperature and field-induced transitions. Considering the dimerization of the chains as the temperature decreases, the first idea that comes to mind is that of the SP transition, sketched in

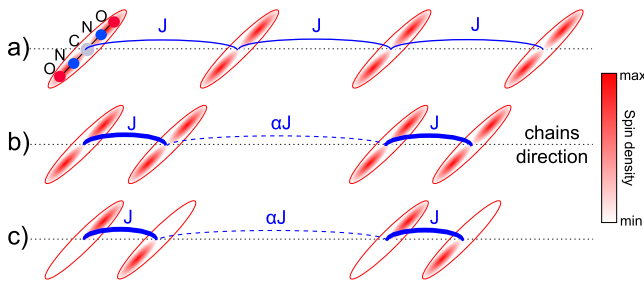


FIG. 4. (Color online) Schematic view of the spin density (dark spots), in the ONCNO^- group (ellipses), along the chains. (a) Uniform chains at $T > T_c$; (b) dimerized chains at $T < T_c$ (spin-Peierls scenario); (c) spin-density ordering in dimerized chains at $T < T_c$.

Figs. 4(a) and 4(b). But the latter is predicted to be second-order type,⁹ contrary to our observation in D-F₅PNN. Nevertheless, such a first-order transition has been reported in several molecular compounds, qualified as SP-like systems (see, e.g., Ref. 21). A more puzzling problem is the nonobservation of the incommensurate soliton lattice, predicted above H_{c1} in a SP system. As can be seen in the inset of Fig. 2, the superlattice peak vanishes above H_{c1} instead of splitting into two satellites, and the crystallographic structure was found to be the same as above T_c in zero field. Last, in the standard SP transition theory, the following BCS-type relation is expected:⁹ $2\Delta/k_B T_c = 3.53$. But for D-F₅PNN, this ratio is larger than 6, which is not consistent with the conventional SP theory.

Such a large ratio reminds the case of NaV_2O_5 , for which $2\Delta/k_B T_c \sim 6$,²² and suggests that the same scenario could occur in D-F₅PNN: a spin-density ordering, in addition to a

dimerization of the spin chains, as sketched in Fig. 4(c). The transition and the opening of the energy gap at T_c would thus be primarily due to some spin-density ordering, alternatively on the left and on the right of the ONCNO^- group while the dimerization of the chains would play a secondary role. Indeed, such a scenario allowed explain the large $2\Delta/k_B T_c$ ratio in NaV_2O_5 .²² This second scenario seems more likely, but is unfortunately nearly impossible to check experimentally. Determining a spin-density map using polarized neutron diffraction cannot be performed in such low magnetic field ($H_{c1} \sim 1$ T) while measuring the Q dependence of the inelastic structure factor over a few Brillouin zones, as was done in NaV_2O_5 ,²² is not feasible here since the signal is already very small in the first Brillouin zone. Thus, some theoretical work is now needed to test this scenario (regarding the amplitude of dimerization and alternation) or propose another one.

Applying a magnetic field at $T = 50$ mK makes the chains evolve from alternating to uniform. Such a behavior is rather puzzling and deserves theoretical support. It also raises the question of the nature of the FIMO, expected from specific-heat measurements¹³ for $T \leq 0.25$ K, between H_{c1} and H_{c2} .

In conclusion, our combined elastic and INS measurements evidence a “mirror behavior” between decreasing temperature (in zero field) and increasing field (at $T = 50$ mK) in a spin-1/2 AF chain: the system evolves between uniform chains in $C2/c$ space group and alternating chains in Pc space group.

We thank M. Houzet, V. Simonet, and E. Ressouche for fruitful discussions and J. Rodriguez-Carvajal for his help in the structural refinement. Part of this work was supported by the French ANR project NEMSICOM.

*Corresponding author; grenier@ill.fr

¹T. Giamarchi *et al.*, *Nat. Phys.* **4**, 198 (2008) and references therein.

²V. O. Garlea *et al.*, *Phys. Rev. Lett.* **98**, 167202 (2007).

³Ch. Rüegg *et al.*, *Nature (London)* **423**, 62 (2003).

⁴B. Grenier *et al.*, *J. Magn. Magn. Mater.* **310**, 1269 (2007).

⁵V. N. Glazkov, A. I. Smirnov, H. Tanaka, and A. Oosawa, *Phys. Rev. B* **69**, 184410 (2004).

⁶A. Zheludev *et al.*, *Phys. Rev. B* **69**, 054414 (2004).

⁷M. Hagiwara *et al.*, *Phys. Rev. Lett.* **94**, 177202 (2005).

⁸B. Grenier, Y. Inagaki, L. P. Regnault, A. Wildes, T. Asano, Y. Ajiro, E. Lhotel, C. Paulsen, T. Ziman, and J. P. Boucher, *Phys. Rev. Lett.* **92**, 177202 (2004).

⁹A. I. Buzdin and L. N. Bulaevskii, *Sov. Phys. Usp.* **23**, 409 (1980).

¹⁰For a review, see J. P. Boucher and L. P. Regnault, *J. Phys. I* **6**, 1399 (1996).

¹¹M. Takahashi *et al.*, *Mol. Cryst. Liq. Cryst.* **306**, 111 (1997).

¹²A. Zheludev *et al.*, *J. Am. Chem. Soc.* **116**, 2019 (1994).

¹³Y. Yoshida *et al.*, *Physica B* **329-333**, 979 (2003).

¹⁴Y. Yoshida *et al.*, *J. Magn. Magn. Mater.* **310**, 1215 (2007).

¹⁵N. Sakai *et al.* (unpublished).

¹⁶Y. Yoshida (unpublished).

¹⁷J. Rodriguez-Carvajal, *Physica B* **192**, 55 (1993).

¹⁸The atomic coordinates and Debye-Waller factors resulting from the refinement will be published elsewhere.

¹⁹The distances from molecule A to B and B to A' were calculated using the position of the C1 atom in each molecule, obtained from the structural refinement.

²⁰A. B. Harris, *Phys. Rev. B* **7**, 3166 (1973).

²¹W. Fujita and K. Awaga, *Science* **286**, 261 (1999).

²²B. Grenier, O. Cepas, L. P. Regnault, J. E. Lorenzo, T. Ziman, J. P. Boucher, A. Hiess, T. Chatterji, J. Jegoudez, and A. Revcolevschi, *Phys. Rev. Lett.* **86**, 5966 (2001).